

## Accomplishments under ARM Support for FY2008–2011

**Project ID:** 0014374

**Award #:** ER64562

**Project:** Use of the ARM Measurements of Spectral Zenith Radiance for Better Understanding of 3D Cloud-Radiation Processes & Aerosol-Cloud Interaction

**PI:** Dr. Alexander Marshak, Dr. Warren Wiscombe

**Co-Is:** Dr. Yuri Knyazikhin, Dr. Christine Chiu

### 1. Project Goals

We proposed a variety of tasks centered on the following question: what can we learn about 3D cloud-radiation processes and aerosol-cloud interaction from rapid-sampling ARM measurements of spectral zenith radiance? These ARM measurements offer spectacular new and largely unexploited capabilities in both the temporal and spectral domains. Unlike most other ARM instruments, which average over many seconds or take samples many seconds apart, the new spectral zenith radiance measurements are fast enough to resolve natural time scales of cloud change and cloud boundaries as well as the transition zone between cloudy and clear areas. In the case of the shortwave spectrometer, the measurements offer high time resolution and high spectral resolution, allowing new discovery-oriented science which we intend to pursue vigorously. Research objectives are, for convenience, grouped under three themes:

- Understand radiative signature of the transition zone between cloud-free and cloudy areas using data from ARM shortwave radiometers, which has major climatic consequences in both aerosol direct and indirect effect studies.
- Provide cloud property retrievals from the ARM sites and the ARM Mobile Facility for studies of aerosol-cloud interactions.
- Assess impact of 3D cloud structures on aerosol properties using passive and active remote sensing techniques from both ARM and satellite measurements.

### 2. Overview

We have basically completed all the goals stated in the previous proposal and published or submitted journal papers thereon. Our group published 26 papers during this proposal period. In section 3, we highlight some of those papers; a complete list is given in section 4.

### 3. Highlights (References to cited papers are given in [])

(1) **ARM SWS data are used to study cloudy-clear transition zone [9].** To the naked eye, clouds appear to have sharp boundaries. But cloud boundaries are actually somewhat fuzzy. Fuzzy cloud boundaries create major headaches for studies of aerosol indirect effect and aerosol radiative forcing – especially when, as with most satellite instruments, spatial resolution is too poor to resolve the transition zone. Recently, one-sec-resolution data from the shortwave spectrometer (SWS) provide a unique opportunity to analyze the transition zone. In Fig. 1 we demonstrated a remarkable linear relationship in the transition zone between the sum and difference of radiances at 870 and 1640 nm wavelengths. The intercept of the relationship is mostly determined by aerosol optical depth, while the slope is mostly determined by cloud droplet size. This linearity could be predicted from simple theoretical considerations and furthermore supported the inhomogeneous mixing hypothesis.

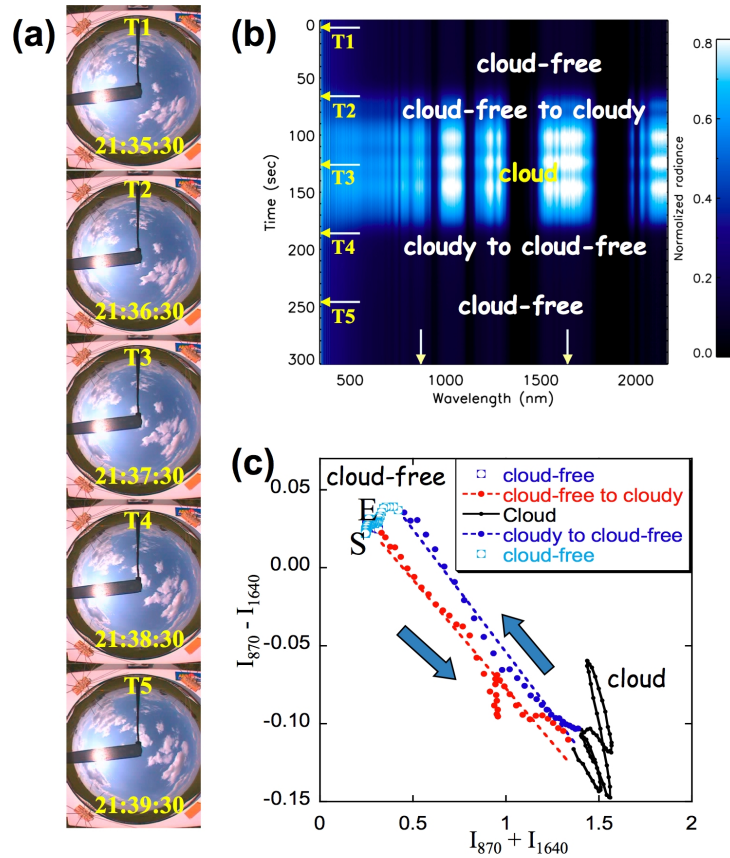


**Fig. 1.** (a) Total sky images on 18 May 2007, and (b) plot of SWS normalized zenith radiances. In (b), arrows pointed at the time axis correspond to the times of the images shown in (a), while arrows pointed at the wavelength axis correspond to 870 and 1640 nm. (c) is the plot of radiance difference vs. sum at 870 and 1640 nm. Letters S and E indicate the start and end of the time series. Two arrows show the flow of time evolution. A remarkable linear relationship is found in the transition zone.

(2) **In the cloudy-clear transition zone a spectral invariance behavior was found in ARM zenith radiance spectra [12, 20, 23, 24],** as shown in Fig. 2. This behavior suggests that the spectral signature of the transition zone is a linear mixture between the two extremes (definitely cloudy and definitely clear). The weighting function of the linear mixture is a wavelength-independent characteristic of the transition zone. An important result of these discoveries is that high temporal resolution radiance measurements in the clear-to-cloud transition zone can be well approximated by lower temporal resolution measurements plus linear interpolation. Also, our radiative transfer calculations suggest that the spectrally-invariant relationship is mainly determined by cloud properties, and is insensitive to aerosol properties and the underlying surface type.

The “spectrally-invariant relationships” are the consequence of wavelength independence of the extinction coefficient and scattering phase function in vegetation. This wavelength-independence does not in general hold in the atmosphere, but in cloud-dominated atmospheres the total extinction and total scattering phase function are only weakly sensitive to wavelength. In two companion papers [23, 24] we discussed the analogy between cloud and vegetation remote sensing, identified the atmospheric conditions under which the spectrally-invariant approximation can accurately describe the extinction and scattering properties of cloudy atmospheres and tested validity of the assumptions and accuracy of the approximation with 1D radiative transfer calculations using DISORT and SBDART. It was shown that, for cloudy atmospheres with cloud optical depth above 3, and for spectral intervals that exclude strong water vapor absorption, the spectrally-invariant relationships found in vegetation-canopy radiative transfer are valid to better than 5%. The physics behind this phenomenon, its mathematical basis, and possible applications to remote sensing and climate were discussed. This is the first step towards theoretical justification of a spectrally-invariant relationship recently found in ARM shortwave spectrometer observations and confirmed by SBDART simulations in [12] and [20].

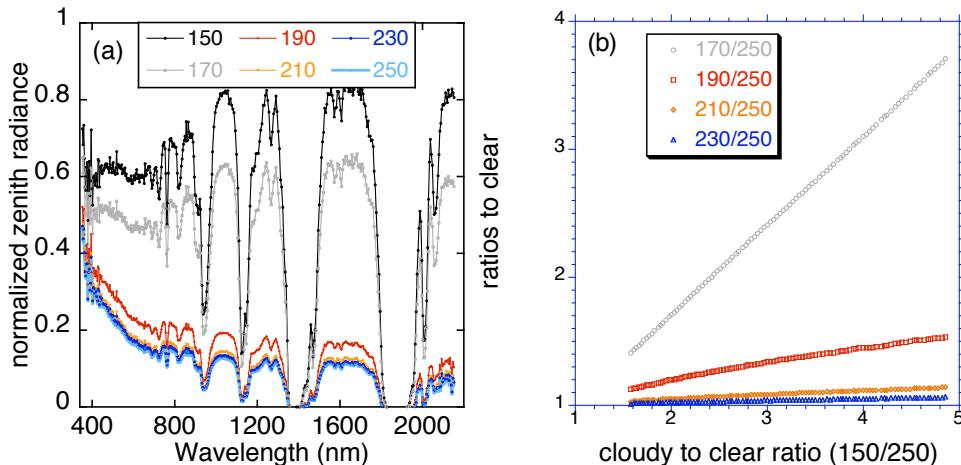


**Fig. 2.** (a) Normalized SWS zenith radiance spectrum measured on 18 May 2007 from 150 s (cloudy) to 250 s (clear) with 20s interval. (b) Ratios of zenith radiance at wavelengths from 350 to 1800 nm, excluding water vapor absorption bands.

(3) **Pioneering work on cloud property retrievals [13, 19]** has attracted favorable notice well within and outside the ARM community. Cloud property retrievals from our group have been used for aerosol-cloud interaction studies [13]. Using data from the ARM Mobile Facility deployment at Point Reyes, CA in 2005, we have characterized and found that aerosol-cloud interactions varied depending on the environmental conditions and observational approaches, such as 1) the assumption of constant cloud liquid water path (LWP), 2) the relative value of cloud LWP, 3) methods for retrieving cloud drop number concentration, 4) aerosol size distribution, 5) updraft velocity, and 6) the scale and resolution of observations.

NASA AERONET has adopted our methods and operated sunphotometers in “cloud mode”, promising the first worldwide observation of cloud optical depth from the ground (Fig. 3). We tested cloud property retrievals at the ARM Oklahoma site for a variety of situations. For overcast cases, 1.5-min average cloud-mode optical depth retrievals agreed to better than 15% with those from MFRSR. For broken clouds, our retrievals could capture the rapid variations revealed by the MWR. A three-year climatology of cloud-mode retrievals agreed well with cloud radar retrievals in both seasonal variation and occurrence distribution.

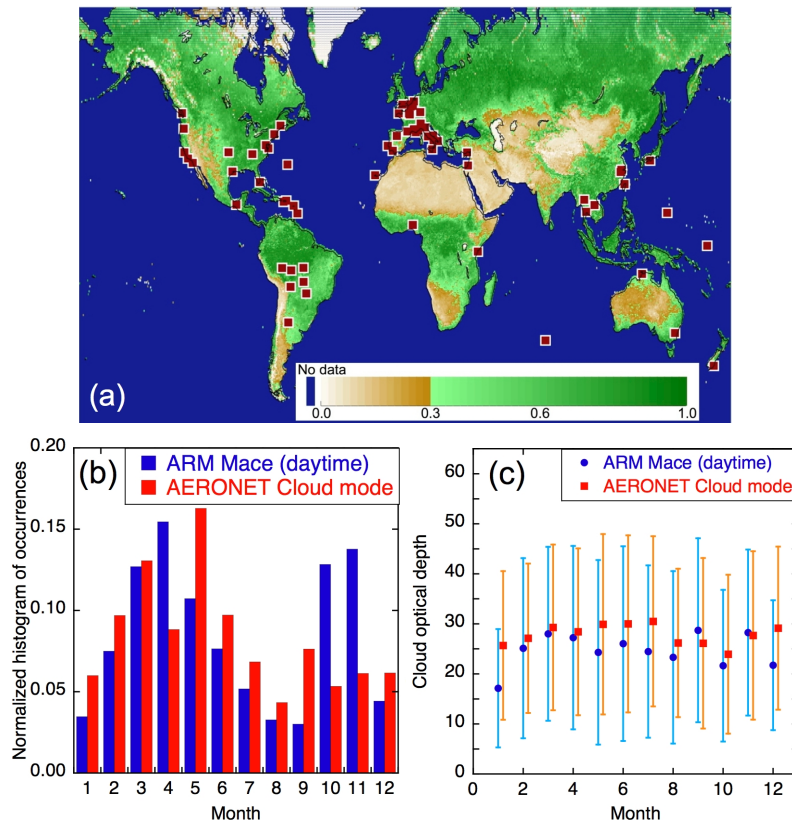


**Fig. 3.** NASA AERONET has adopted our methods and operated sunphotometers in “cloud mode”. (a) Potential cloud mode site locations in AERONET. (b) Normalized histogram of occurrence for overhead cloudiness at the ARM SGP. Blue bars represent occurrences of Mace’s retrievals during years 2002–2004, while red bars represent occurrences of AERONET retrievals during Nov 2004 – Jun 2008. (c) Monthly average cloud optical depth with one standard deviation.

(4) **New stochastic cloud models have been developed [14, 16, 17]**, which is useful for studying 3D radiative transfer features of broken cumulus clouds and for better understanding of shortwave radiation and interpretation of the remote sensing retrievals. The model in [14] used an autocorrelation function of the cloud indicator field and a distribution of cloud layer thickness, as input parameters. A numerical algorithm is based on spectral models of homogeneous random fields. As shown in Fig. 4, the algorithm output is statistical realizations of cloud optical depth and cloud top height fields with approximately the same correlation and joint distribution functions as the original ones. This model can be freely downloaded from [http://i3rc.gsfc.nasa.gov/Public\\_codes\\_clouds.htm](http://i3rc.gsfc.nasa.gov/Public_codes_clouds.htm).

We also developed a new analytical statistical model and compared its statistics with those from large-eddy simulations (LES) [16, 17]. The model depends on two parameters (cell size and occupancy probability) and provides chord distributions of clouds and gaps between them by length, as well as the cloud fraction distribution. Our approach is based on the assumption that the structure of a cloud field is determined by a semi-regular grid of cells, which are filled with cloud with some probability. We start with a simple discrete model, where clouds and gaps can occupy an integer number of cells, and then develop its continuous analog allowing for arbitrary cloud and gap sizes.

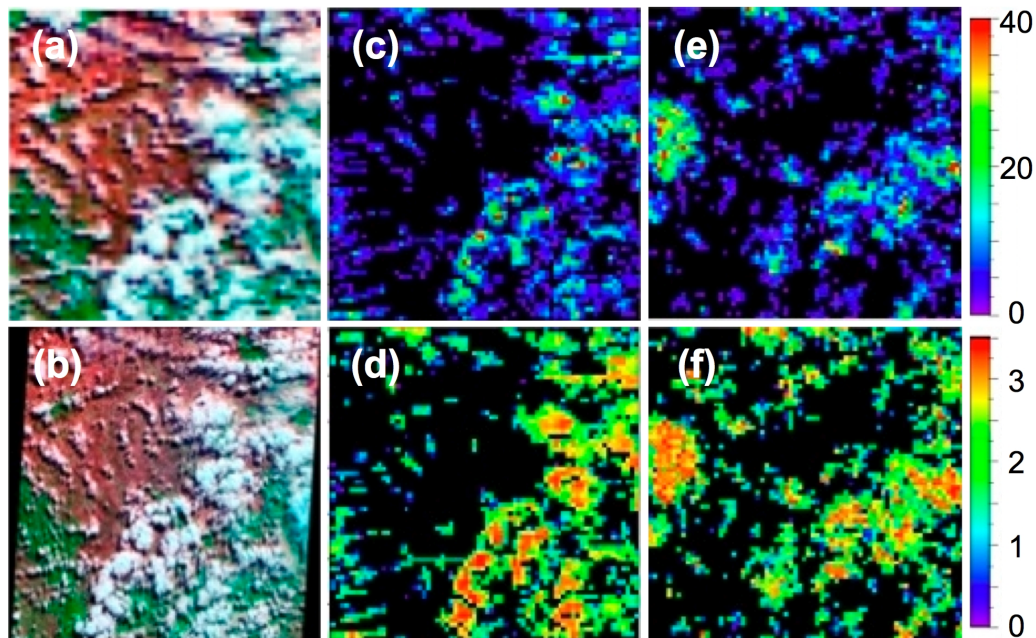


**Fig. 4.** A 68 km by 68 km region in Brazil centered at 17°S and 42°W collected on August 9, 2001 at 1015 local time by (a) MODIS with 1 km resolution and (b) ASTER with 15 m resolution. (c) and (d) are cloud optical depth and (d) cloud top height (in km) retrieved from MODIS, while (e) and (f) are one realization from a stochastic model.

(5) **Cloud-side remote sensing [8]** approach has been thoroughly checked for the retrievals of profiles of cloud thermodynamic phase and effective radius, indicating a promising scanning approach for ground-based measurements. In contrast to the plane-

parallel approximation, 3D radiative transfer is used for interpreting observed reflectances. To retrieve the information about droplet size, we used the probability density function of the droplet size distribution and its first two moments instead of the assumption about fixed values of the droplet effective radius. The proposed Bayesian retrieval algorithm used a database that combined a large number of cloud data sets and related simulated reflectances. Figure 5 shows one example of cloud field from the state-of-the-art Goddard Cumulus Ensemble model and corresponding retrievals of droplet size vertical profiles, showing a promising scanning approach for both ground-based and satellite measurements.

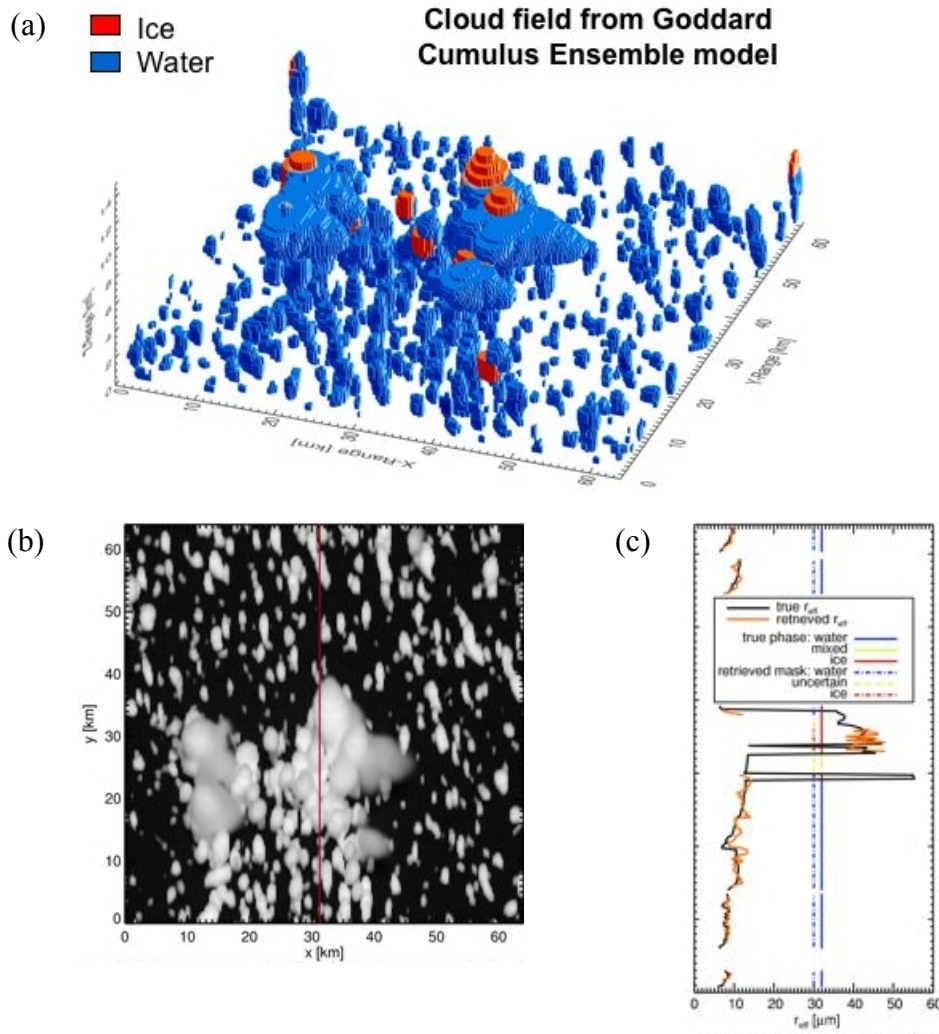


**Fig. 5.** (a) 3-D distribution of LWC (blue) and IWC (red) for the test cloud data set. (b) Related simulated observation of  $0.87\mu\text{m}$  reflectance for  $60^\circ$  viewing zenith and  $45^\circ$  solar zenith angle. (c) Profiles of retrieved cloud effective radius

**(6) Impact of clouds on aerosol retrievals [4, 6],** due to the enhanced illumination of cloud-free columns in the vicinity of clouds, is quantified by a simple model. This model is based on the assumption that the enhancement in the cloud-free column radiance

comes from enhanced Rayleigh scattering that results from the presence of the nearby clouds (as shown in Fig. 6). This assumption leads to a larger increase of AOT for shorter wavelengths, or to a “bluing” of aerosols near clouds. The enhancement in Rayleigh scattering is estimated using a stochastic cloud model to obtain the radiative flux reflected by broken clouds and comparing this flux with that obtained with the molecules in the atmosphere causing extinction, but no scattering.

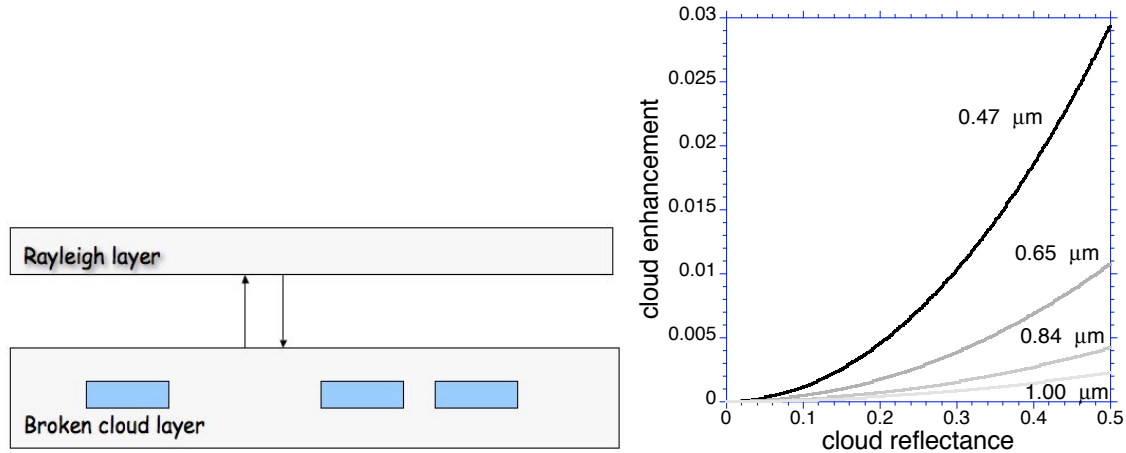


**Fig. 6.** (left) A schematic two-layer model of a broken cloud field (lower layer) and Rayleigh scatterers (upper layer). (right) Cloud-induced enhancement as a function of cloud reflectance for four wavelengths: 0.47, 0.65, 0.84, and 1.00 μm.

**(7) Impact of clouds on aerosol retrievals is also studied using MODIS and CALPSO data [15, 25, 26].** By analyzing a large dataset of MODIS observations over the Northeast Atlantic Ocean, we examined the effect of 3D radiative interactions between clouds and their surroundings [15]. The results indicate that 3D effects are responsible for a large portion of the observed increase, which extends to about 15 km away from clouds. This implies that it is important to consider 3D radiative effects in interpretation of solar reflectance measurements over clear regions in the vicinity of clouds.

To further confirm the impact of 3D radiative effects on aerosol retrievals, a statistical analysis of a month long global dataset of CALIPSO lidar observations over oceans is presented in [25]. The results showed that the transition zone between clouds and cloud-free areas occurs below cloud top level and is ubiquitous over all oceans, and also that the zone extends as far as 15 km away from clouds. Figure 7 indicates that aerosol particle sizes increase near clouds; this increase is a global phenomenon and the overall trend is neither caused by a single dominant region nor is it an artifact of combining observations from vastly different regions of the Earth. Our results underline the need for caution to avoid biases in studies of satellite aerosol products, aerosol-cloud interactions, and aerosol direct radiative effects.

In paper [26] we revisited CALIPSO aerosol backscatter enhancement in the transition zone with particular attention to effects of data selection based on the confidence level of

cloud-aerosol discrimination (CAD). We showed that backscatter behavior in the transition zone strongly depends on the CAD confidence level. Higher confidence level data has a flatter backscatter far away from clouds and a much sharper increase near clouds (within 4 km), thus a smaller transition zone. With the highest confidence level data, approximately a 27% increase of aerosol backscatter coefficient within a distance of 5 km to clouds is estimated, which is comparable to a previous airborne lidar measurement. In addition, the overall enhancement is more pronounced for small clear-air segments and horizontally larger clouds.

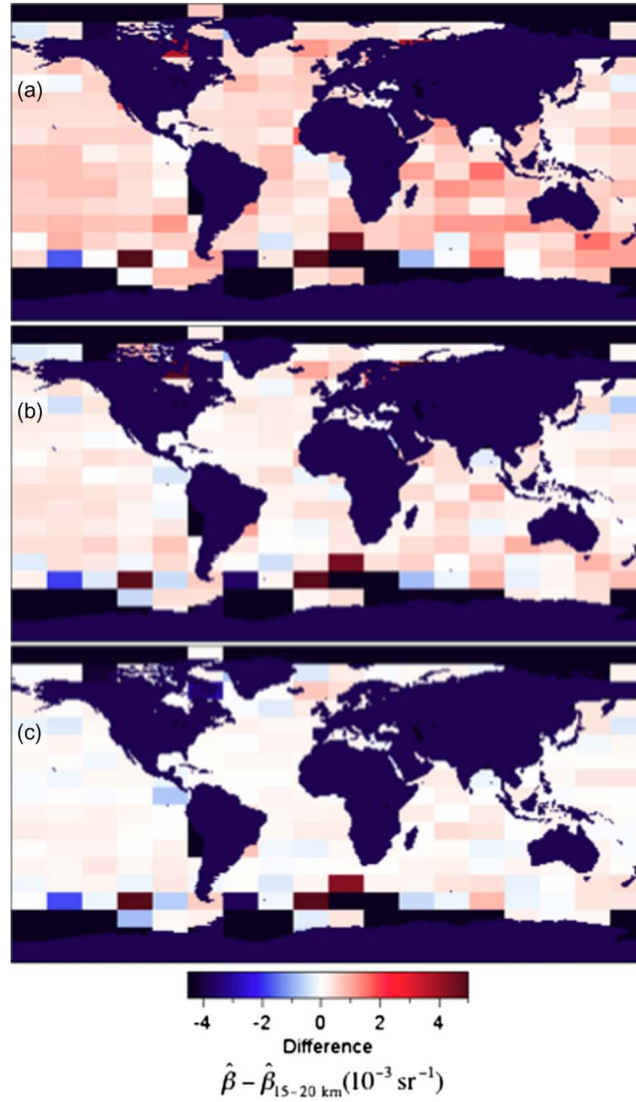


**Fig. 7.** Map of difference between median vertically integrated 532-nm backscatter values  $\hat{\beta}$  at different distance from the nearest cloud, indicating that aerosol particle sizes increase near clouds and this increase is a global phenomenon. (a)  $\hat{\beta}_{0-5km} - \hat{\beta}_{15-20km}$ . (b)  $\hat{\beta}_{5-10km} - \hat{\beta}_{15-20km}$ . (c)  $\hat{\beta}_{10-15km} - \hat{\beta}_{15-20km}$ .



**(8) Improvement of cloud optical depth retrievals using multiangular measurements [2].** In Paper [2] we used large LES for Sc, small trade Cu and land surface-forced fair weather Cu. Reflectances in multiple directions were computed using 3D radiative transfer. Neural networks were trained to retrieve the mean and standard deviation of simulated reflectances. We found only small improvements in the retrievals of Cu cloud optical depth, that suggest that measurements of solar reflection in multiple directions do not contribute substantially to more accurate optical depth retrievals for Cu. The 3D statistical retrievals, however, even with only the nadir camera, proved to be more accurate for small Cu than standard nadir plane-parallel retrievals and therefore this approach is worth pursuing.

**(9) Parameterization of canopy 3D structure for climate models and remote sensing applications can be improved from ARM hyperspectral radiation flux data [1, 3].** A new approach is introduced in [1] to account for 3D effects in a shortwave radiation block for the use in the CLM (Common Land Model) which is a part of the NCAR climate model. This block evaluates how much radiation is absorbed by canopies and their underlying surfaces. It was shown that *the canopy spectral invariants* are required to account for the effect of 3D canopy structure on canopy reflective and absorptive properties. These parameters can be directly derived from ARM hyperspectral radiation fluxes acquired over vegetated surfaces as was demonstrated in our ARM poster (<http://www.arm.gov/publications/proceedings/conf17/poster/P00081.pdf>) and publication (Schull et al. *Geophys. Res. Lett.*, 34, doi:10.1029/2007GL031143, 2008). Paper [3] discusses a stochastic approach to parameterize canopy structure for remote sensing applications.

**(10) ARM observations are included as example in review papers on atmospheric radiation and light scattering for physicists [10, 21].** In the invited chapter 7 in “*Light Scattering Reviews*” monograph [10], we covered many aspects of the diffusion-theoretical approach for in situ detectors as well as remote cloud observations. We also discussed applications to current and futuristic cloud remote sensing technologies from ground-level, airborne and space-based platforms. Both active (lidar) and passive (especially, oxygen A-band spectroscopic) modalities are described.

In the invited review paper [21] for *Reports on Progress in Physics* we surveyed the 3D atmospheric radiative transfer literature over the past 50 years and identifies three concurrent and intertwining thrusts: first, how to assess the damage (bias) caused by 3D effects in the operational 1D radiative transfer models and second, how to mitigate this damage? Finally, paper discussed of how to exploit 3D radiative transfer phenomena to innovate observation methods and technologies.

#### 4. Publication list

(Members of our science team are in bold)

##### **2008**

- [1] Dickinson, R.E., L. Zhou, Y. Tian, Q. Liu, T. Laverigne, B. Pinty, C. B. Schaaf, and Y. **Knyazikhin**, 2008: A 3-dimensional analytic model for the scattering of a spherical bush, *J. Geophys. Res.*, 113, D20113, doi:10.1029/2007JD009564.
- [2] Evans, K.F., A. **Marshak**, and T. Varnai, 2008: The potential for improved cloud optical depth retrievals from the multiple directions of MISR. *J. Atmos. Sci.*, 65, 3179-3196.
- [3] Huang, D., **Knyazikhin**, Y., Wang, W., Deering, D. W., Stenberg, P., Shabanov, N., & Myneni, R.B., 2008: Stochastic transport theory for investigating the three-dimensional canopy structure from space measurements, *Remote Sens. Environ.*, 112, 35-50.
- [4] **Marshak**, A., G. Wen, J.A. Coakley, L.A. Remer, N.G. Loeb, and R.F. Cahalan, 2008: A simple model of the cloud adjacency effect and the apparent bluing of aerosols near clouds. *J. Geophys. Res.*, 113, D14S17, doi: 10.1029/2007JD009196.
- [5] Prigarin, S.M. and A.L. **Marshak**, 2008: Simulation of vector semibinary homogeneous random fields and modeling of broken clouds. *Numeric. Anal. Appl.*, 3, 285-292.
- [6] Wen, G., A. **Marshak**, and R. F. Cahalan, 2008: Importance of Molecular Rayleigh Scattering in the Enhancement of Clear Sky Radiance in the Vicinity of Boundary Layer Cumulus Clouds. *J. Geophys. Res.*, 113, D24207, doi:10.1029/2008JD010592.
- [7] Yang Y., A. **Marshak**, J.C. **Chiu**, W.J. **Wiscombe**, S.P. Palm, A.B. Davis, D.A. Spangenberg, L. Nguyen, J.D. Spinhirne, and P. Minnis, 2008: Retrievals of cloud optical depth from the Geoscience Laser Altimeter System (GLAS) by calibration of solar background signal. *J. Atmos. Sci.*, 65, 3513-3527, doi: 10.1175/2008JAS2744.1
- [8] Zinner, T., A. **Marshak**, S. Lang, J.V. Martins, and B. Mayer, 2008: Remote sensing of cloud sides of deep convection: towards a three-dimensional retrieval of cloud particle size profiles. *Atmos. Chem. Phys.*, 8, 4741-4757.

##### **2009**

- [9] **Chiu**, J. C., A. **Marshak**, Y. **Knyazikhin**, P. Pilewskie, and W. J. **Wiscombe**, 2009: Physical interpretation of the spectral radiative signatures in the transition zone between cloud-free and cloudy regions. *Atmos. Chem. Phys.*, 9, 1419-1430.
- [10] Davis A.B., I.N. Polonski, and A. **Marshak**, 2009: Space-time Green functions for diffusive radiation transport, in application to active and passive cloud probing. In: A.A. Kokhanovsky, [Ed], "*Light Scattering Reviews Vol. 4. Single Light Scattering and Radiative Transfer*", Springer, pp. 169-292.
- [11] Kato, S. and A. **Marshak**, 2009: Solar zenith and viewing geometry dependent errors in satellite retrieved cloud optical thickness; Marine stratocumulus case. *J. Geophys. Res.* 114, D01202, doi:10.1029/2008JD010579.

- [12] **Marshak**, A., Y. **Knyazikhin**, C. **Chiu**, and W. **Wiscombe**, 2009: Spectral invariant behavior of zenith radiance around cloud edges observed by ARM SWS. *Geoph. Res. Lett.*, 36, L16802, doi:10.1029/2009GL039366.
- [13] McComiskey, A., G. Feingold, A. S. Frisch, D. Turner, M. Miller, J. C. **Chiu**, Q. Min, and J. Ogren, 2009: An assessment of aerosol-cloud interactions in marine stratus clouds based on surface remote sensing. *J. Geophys. Res.* doi:10.1029/2008JD011006.
- [14] Prigarin, S. and A. **Marshak**, 2009: A simple stochastic model for generating broken cloud optical depth and cloud top height fields. *J. Atmos. Sci.*, 66, 92-104.
- [15] Varnai, T., and A. **Marshak**, 2009: MODIS observations of enhanced clear sky **reflectance** near clouds. *Geophys. Res. Lett.* 36, L06807, doi:10.1029/2008GL037089.

## **2010**

- [16] Alexandrov, M.D., A. **Marshak**, and A.S. Ackerman, 2010: Cellular statistical models of broken cloud fields. Part I: Theory. *J. Atmos. Sci.*, 67, 2125-2151, doi:10.1175/2010JAS3364.1.
- [17] Alexandrov, M.D., A.S. Ackerman and A. **Marshak**, 2010: Cellular statistical models of broken cloud fields. Part II: Comparison with dynamical model, statistics of diverse ensembles. *J. Atmos. Sci.*, 67, 2152-2170, doi:10.1175/2010JAS3365.1.
- [18] Betts, A. K. and J. C. **Chiu**, 2010: Idealized model for changes in equilibrium temperature, mixed layer depth and boundary layer cloud over land in a doubled CO<sub>2</sub> climate. *J. Geophys. Res.*, 115, D19108, doi:10.1029/2009JD012888.
- [19] **Chiu**, J.C., C.-H. Huang, A. **Marshak**, I. Slutsker, D.M. Giles, B.N. Holben, Y. **Knyazikhin**, and W.J. **Wiscombe**, 2010: Cloud optical depth retrievals from the Aerosol Robotic Network (AERONET) cloud mode observations. *J. Geophys. Res.*, 115, D14202, doi:10.1029/2009JD013121.
- [20] **Chiu**, J.C., A. **Marshak**, Y. **Knyazikhin**, and W.J. **Wiscombe**, 2010: Spectral invariant behavior of zenith radiance around cloud edges simulated by radiative transfer. *Atmos. Chem. Phys.*, 10, 11295-11303, doi:10.5194/acp-10-11295-2010.
- [21] Davis, A.B. and A. **Marshak**, 2010: Solar radiation transport in the cloudy atmosphere: A 3D perspective on observations and climate impacts. *Reports on Progress in Phys.*, 73, doi:10.1088/0034-4885/73/2/026801.
- [22] **Marshak**, A., Y. **Knyazikhin**, C. **Chiu**, and W. **Wiscombe**, 2010: Observed spectral invariant behavior of zenith radiance in the transition zone between cloud-free and cloudy regions. In, *Hyperspectral Image and Signal Processing: Evolution in Remote Sensing* (WHISPERS), 2010 2nd Workshop on (pp. 1-3). Reykjavik, Iceland: IEEE, doi: 10.1109/WHISPERS.2010.5594958.

## **2011**

- [23] **Knyazikhin**, Y., M.A. Schull, L. Xu, R.B. Myneni, and A. Samanta, 2011: Canopy spectral invariants. Part 1: A new concept in remote sensing of vegetation. *J. Quant. Spectr. Radiat. Transfer*, 112, 727-735.

- [24] **Marshak**, A., Y. **Knyazikhin**, C. **Chiu**, and W. **Wiscombe**, 2011: Spectrally-invariant approximation within atmospheric radiative transfer. *J. Atmos. Sci.*, (submitted Feb 2011).
- [25] Varnai, T. and A. **Marshak**, 2011: Global CALIPSO observations of aerosol changes near clouds. *Geosci. Remote Sens. Lett.*, 8, 19-23.
- [26] Yang W., A. **Marshak**, Varnai, T., and Z. Liu, 2011: Effect of CALIPSO cloud aerosol discrimination (CAD) confidence levels on the observation of aerosol properties near cloud. *IEEE Trans. Geosci. Remote Sens.*, (submitted Nov 2010)